IMPROVEMENT OF THE WEATHER RESEARCH AND FORECASTING (WRF) MODEL FOR SOLAR RESOURCE ASSESSMENTS AND FORECASTS UNDER CLEAR SKIES

José A. Ruiz-Arias
NCAR/MMM, Boulder, CO
University of Jaén, Jaén, Spain
jararias@ujaen.es

Christian A. Gueymard
Solar Consulting Services, Colebrook, NH
Chris@SolarConsultingServices.com

Jimy Dudhia
NCAR/MMM, Boulder, CO
dudhia@ucar.edu

David Pozo-Vázquez
University of Jaén, Jaén, Spain
dpozo@ujaen.es

ABSTRACT

A new capability for ingesting gridded aerosols data into the Weather Research and Forecasting (WRF) mesoscale model is being developed. The aim is to improve the shortwave downward solar radiation assessment and forecasting by equipping the model with a mechanism to ingest both high temporal and high spatial resolution aerosol data. This results in a reduction of the bias caused by any misrepresentation of the aerosol optical properties and their spatio-temporal variability. The main impact of this improvement is on the direct and diffuse components of solar radiation. We present here a preliminary study over the Continental United States using the Goddard Space Flight Center shortwave scheme, MODIS Level 3 aerosol optical depth data, and three ground stations of NOAA's SURFRAD radiation network. Results under cloudless conditions showed a relative improvement in the mean bias error of about 80% in the direct normal irradiance and up to about 70% in the diffuse irradiance, with respect to the model's run without aerosols, which is currently WRF's default operation mode.

1. INTRODUCTION

With the current worldwide increase in the number of solar applications, accurate estimates of the solar resource available at the ground surface become critical. Since the solar resource is variable, its forecasts are also essential for an optimal operation of solar power plants, and for the stability of the electric grids into which they are connected. Solar forecasts also have the potential to facilitate a higher penetration of solar electricity generation in the energy mix, and to maximize investment revenues.

Currently, satellite-based models are considered the most reliable methodology for solar resource assessment under all-sky conditions. They have also demonstrated their skills in solar radiation nowcasting (forecast up to ≈6 hours ahead). However, they are not exempt from drawbacks. For instance, these models do not offer reliable forecasts beyond the nowcast 6-hour limit, while their modeled datasets are limited in space and time by the availability of proper satellite imagery.

Numerical Weather Prediction (NWP) models provide a comprehensive and physically-based state-of-the-art description of the atmosphere and its interactions with the Earth surface. Regional Climate Models (RCM) have been specially devised to downscale, over a limited area of interest, the coarse description of the atmosphere produced with a Global Circulation Model. They are routinely used worldwide to produce weather forecasts several days ahead, but can also be used to describe the atmosphere at an enhanced spatial and temporal resolution, based on any of the numerous and decades-long atmospheric reanalyses now available. The downscaling procedure takes care of local surface-related effects (i.e., terrain topography, sea influence, urban environment, etc.) that occur at sub-grid scale in the coarser resolution of the reanalysis. Therefore, RCMs constitute a very promising tool for solar resource assessment and forecasting. However, as with the satellite-based methods, they still need further development to respond to the specific requirements of the solar industry.

Traditionally, the physical processes involved in NWP models and their applications have only required the global horizontal irradiance (GHI), so that these models usually do not provide (at least publicly) the direct component, which is required, for instance, for current concentrating solar energy/power applications and for an improved representation of the surface energy fluxes over complex terrains. Additionally, in spite of the key role that aerosols play in the attenuation of solar radiation, their effect has most often been oversimplified in NWP, GCM and RCM models. This deficient modeling generally tends to overestimate the solar resource. So

far, the lack of precise aerosol modeling in NWP models has been mostly due to insufficient aerosol data. This has resulted in the use of simple monthly climatologies, or even in the complete neglect of aerosols. Recently, Cebecauer et al. [1] showed the benefits of assessing the higher values of solar radiation using daily updates of aerosol optical depth (AOD) instead of monthly representations. Even more recently, Gueymard [2] showed that, on average, using monthly AOD data rather than daily data captures only about half of their daily variability.

However, in the last few years, the number and time span of the available worldwide aerosol databases have considerably increased, and rapid progress has been made in aerosol science. These developments have been boosted mostly by global ground measurement networks, such as AERONET [3], and by satellite sensors, such as the Moderate Resolution Imaging Spectroradiometer (MODIS) or the Multi-angle Imaging SpectroRadiometer (MISR). In particular, NASA's MODIS instruments have already provided more than 10 years of global aerosol measurements and are still operating. The MODIS Level 3 (L3) [4] product (see Section 3.1) provides global daily estimates of AOD at 550 nm with 1x1° spatial resolution. This high temporal and spatial resolution and the global coverage make the MODIS L3 dataset especially suitable for use with NWP models. Additionally, chemical transport models are another possible source for aerosol forecasts [5]. These new sources of data are particularly appropriate in solar radiation forecast studies when aerosol effects must be addressed.

2. SHORTWAVE SOLAR RADIATION PARAMETERIZATION IN WRF AND CHANGES IN THE CODE

The radiation schemes in WRF are tailored to evaluate the atmospheric heating rate due to both short- and long-wave radiative flux divergences, and to predict the incident radiation needed to calculate the ground heat budget. All current schemes use the independent column approximation, so that each vertical column of the model, where the atmosphere is discretized in several layers, is treated independently. This assumption is good as long as the vertical thickness of the model layers is much less than the horizontal grid length. Shortwave radiation includes wavelengths from the ultraviolet to the infrared through the visible solar spectrum, as well as absorption, reflection, and scattering processes in the atmosphere and at surface. The model-predicted cloud and water vapor distributions, as well as specified carbon dioxide, ozone, and (optionally) trace gas concentrations are also considered [6].

By far, the most frequently used shortwave radiative scheme is the MM5 scheme, also known as Dudhia's scheme [7]. It was taken directly from MM5, the precursor of WRF. It is a simple broadband model, limited in scope to the evaluation of GHI at various vertical layers. However, WRF also has two advanced radiative transfer (two-stream) codes that are very suitable for addressing the assessment of the solar radiation components, including aerosol effects. These two codes are the Goddard Space Flight Center (GSFC) scheme [8] and the Short Wave Rapid Radiative Transfer Model scheme [9]. They use 11 and 14 spectral bands, respectively, from ultraviolet to near-infrared. They calculate the direct effect of aerosols on solar radiation using the main aerosol optical properties (AOD, single-scattering albedo and asymmetry parameter) at each spectral band and each vertical layer of the model.

The current implementation of the shortwave solar radiation schemes in WRF is tailored to calculate the GHI only, and thus does not provide either the direct normal irradiance (DNI) or the diffuse horizontal irradiance (DHI). These two components are much more sensitive to AOD than GHI [2]. In this work, we have expanded the code of the GSFC scheme to evaluate the two components just mentioned, and to include the effects of aerosols. To this end, we have included an aerosol parameterization to create a vertical profile and a spectral distribution of AOD, single-scattering albedo and asymmetry parameter from a gridded estimate of AOD at 550 nm. The vertical profile follows the approach described by Hess et al. [10] using a scale height of 2 km. The spectral disaggregation is based on the approach followed by Gueymard [11] in the SMARTS radiative transfer code. A type of aerosol has to be assumed for these calculations [12], which, in practice, means that a broad and representative size distribution of the aerosol particles is assumed. The size distribution is closely related to the Angström exponent (the higher the Angström exponent, the finer the aerosol particles), which describes the spectral distribution of AOD. Typically, both the size and scattering potential of most aerosol particles increases with moisture. The approach followed here considers this hygroscopic effect by modulating the Angström exponent based on the actual relative humidity. This approach is convenient for two main reasons. Firstly, because the current estimates of the Angström exponent with satellite methods are still very noisy and uncertain [13]. Secondly, because WRF is typically run over a limited area of the Earth, where a predominant type of aerosol can be usually identified. Conversely, assuming a single aerosol model would not be advisable in the case of global model runs.

3. AEROSOL OPTICAL DEPTH DATA

3.1. Gridded Aerosol Optical Depth Data

From the radiances observed by the MODIS sensors aboard the polar-orbiting Terra and Aqua satellites (organized into 5-minute sections, known as granules, each one ~2300 km long), some geophysical aerosol parameters such as spectral AOD at 550 nm and particle size information are derived with an ungridded 10-km nominal resolution at the time of the satellite overpass. This product, known as Level 2 (L2), is produced using

either one of three different algorithms: two over land surfaces (Dark-Target and Deep-Blue, the latter for bright surfaces) and one over oceans. The MODIS L3 product is a global daily aggregation of L2 data into a regular longitude-latitude grid with a spatial resolution of 1x1°. Tropospheric aerosols show significant variability at spatial scales of a few hundred kilometers [14]. Therefore, the MODIS L3 product is a good candidate as a source of gridded AOD in regional weather models, since it combines global coverage with high spatial and temporal resolution. Specifically, the combined land and ocean AOD MODIS L3 product (Collection 5.1) at 550 nm from the Terra satellite is used here. It is derived from the best estimate for both ocean and land with the best quality data (QA confidence flag = 3) from the Terra MODIS L2 dataset.

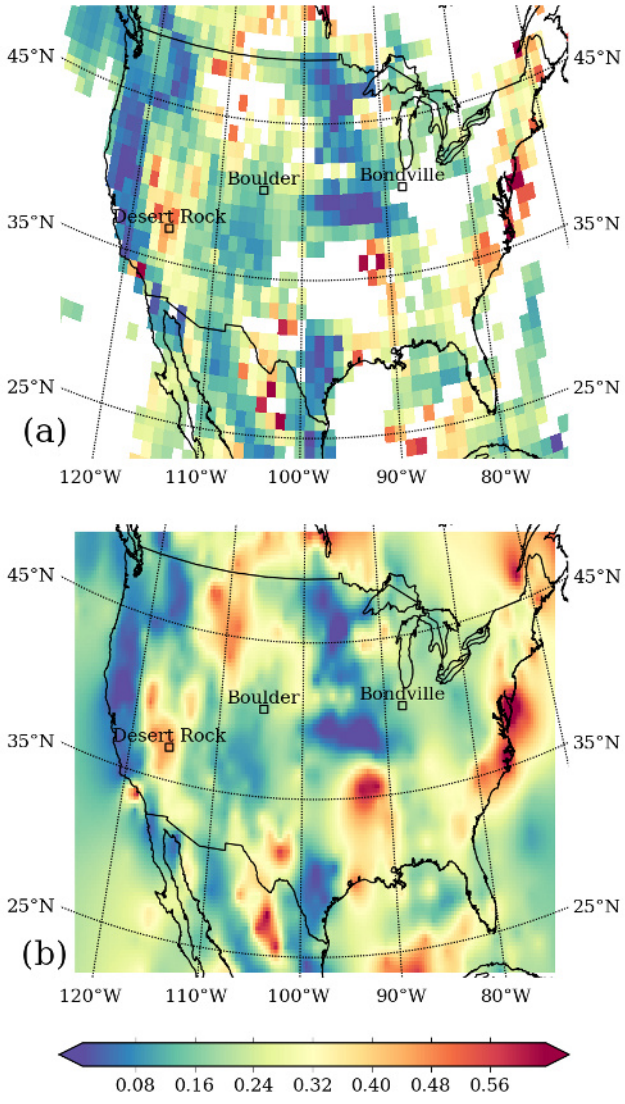

Fig. 1: Gridded AOD at 550 nm from the MODIS L3 dataset on July 27, 2009 over the study region (a); interpolated gridded AOD values from (a) into the simulated WRF domain grid using ordinary kriging (b). White cells are missing values. The square markers show the location of the experimental sites.

Since the retrieval algorithms were designed for cloudless conditions, a cloud screening procedure is applied in the early stages of the retrieval. This screening, as well as other uncertainty sources that flag some pixels as QA<3, produce gaps in the MODIS L2 product, which in turn lead to gaps in the L3 data. These missing cells have to be filled out before AOD data can be used in the NWP model. Additionally, it is well known that regional biases also exist in the MODIS L2 data, which invariably affect the L3 data. Such is the case of the Southwestern U.S. region, where considerable interest for large solar power plants exists. Therefore, a preliminary regional correction of the AOD bias in the satellite estimates is recommended. A very comprehensive global validation of MODIS L2 data is provided by Levy et al. [13].

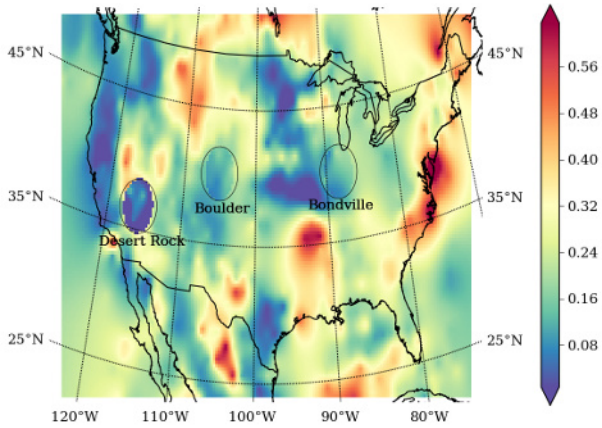

Fig. 2: As Fig. 1b but showing the result of the Cressman analysis scheme at the experimental sites. The circles show the influence radius of the observations

3.2. Ground Measurements

One key aspect of this study is to assess the skill of the GSFC shortwave radiation scheme, as implemented in WRF, to calculate GHI, DNI and DHI, and evaluate how the inclusion of a daily update of the AOD at 550 nm further improves this skill. The experimental dataset used to validate the modeled results should include simultaneous *in-situ* measurements of GHI, DNI, DHI and AOD at 550 nm. Moreover, the solar radiation data must have a high temporal resolution (1 to 5 minutes) so that a reliable cloud-screening algorithm can be applied. NOAA's SURFRAD network (*http://www.srrb.noaa.gov/surfrad/*) complies with these requirements. Currently, seven SURFRAD stations operate in the USA. Among other radiometric quantities, they record DNI, DHI and GHI at high temporal resolution (1-minute since 2009, 3-minute before), as well as ancillary meteorological parameters (surface pressure, relative humidity and 2-meter temperature). For model validation, we have used the summer months of 2009 (June, July and August) at three different locations: Bondville (IL), Boulder (CO) and Desert Rock (NV). These three locations are representative of very

different climatic conditions. The Long and Ackerman [15] cloud screening algorithm was applied to the dataset and 2.6%, 9.2% and 21.3% of the sunup data were flagged as clear-sky for Bondville, Boulder and Desert Rock, respectively.

Even though AOD is monitored with Multifilter Rotating Shadowband Radiometers (MFRSR) at very high temporal resolution (one minute), the automatic cloud-screening procedure in the retrieval algorithm prevents the usability of all existing records. The MFRSR nominal spectral channels are 415, 500, 614, 670, 868 and 940 nm. More information can be found at *http://www.srrb.noaa.gov/surfrad/aod/*. From these spectral measurements the AOD at 550 nm was calculated with Angström's law using AOD data from the 500, 614 and and 868 nm channels.

4. EXPERIMENTAL SET UP

The WRF v3.3 model was run over a 27-km single domain in the Contiguous States from June to August 2009. The atmosphere was discretized into 27 vertical layers. Grid analysis nudging was applied to the horizontal wind components, temperature, moisture and pressure in all layers above the planetary boundary layer. Initial and boundary conditions were taken from the ERA-Interim analysis dataset of the ECMWF [16]. The simulation was restarted every 7 days with 1 day spin-up. The integration time-step of the model was set to 2 minutes, the radiation calculations were done every 10 minutes and the results saved every 10 minutes. The general physical configuration of the model included: microphysics and longwave radiation Goddard schemes, modified Goddard scheme for shortwave solar radiation, Monin-Obukhov similarity for surface layer, Noah land surface model, YSU scheme for planetary boundary layer and Kain-Fritsch convection scheme. Details on these physical options can be found at *http://www.mmm.ucar.edu/wrf/users*.

Three different cases (and thus, three different runs) were considered in parallel: (i) no-aerosol (AOD=0); (ii) rural aerosols (daily updates of AOD); and (iii) urban aerosols (daily updates of AOD). These two types of aerosols coincide with those described by Shettle and Fenn [12]. The aerosol input (AOD at 550 nm) to the mesoscale model was gathered from the daily MODIS L3 dataset. As it still contained remaining data gaps after the averaging procedure from the MODIS L2 dataset, we used Ordinary Kriging (OK) [17] to fill them out for every day of the analyzed period. Figure 1a shows the MODIS L3 daily AOD estimate for July 27, 2009. Note the presence of numerous data gaps. Square markers show the location of the observational sites. Figure 1b shows the resultant gridded aerosol map after using OK with the same grid as the WRF domain used in the simulation.

To really test the skill of the GSFC shortwave scheme, we constrained the sources of uncertainty from the model inputs as much as possible. In such a study, the largest source of uncertainty is cloudiness. This uncertainty encompasses that related to the cloud radiative transfer and that due to cloud location errors in time and space. To evaluate the effects of aerosols more conclusively, we took the conservative approach of restricting our validation study only to cloudless situations. Only those records with cloudless conditions in both the observations and the model were used in the validation procedure. The cloud fraction calculated by WRF was reduced to a 2D field from the values for all the different layers, using a maximum overlapping assumption. The resultant cloud fraction was a binary field: 0 for cloudless conditions, and 1 for cloudy skies. The second source of uncertainty in general, but the most important one under cloudless conditions, is AOD. In the present case, this uncertainty is caused by the bias in the interpolated MODIS L3 data (Fig. 1b). To remove this bias at the validation sites, we used a Cressman analysis scheme [18] to nudge the interpolated AOD grid (AOD_{OK}) to the local measured values (AOD_{obs}) at each site i. The corrected AOD values (AOD_{cr}) where calculated as:

$$AOD_{cr}(j) = AOD_{OK}(j) + \frac{\sum_{i=1}^{n} w(i,j)\left[AOD_{obs}(i) - AOD_{OK}(i)\right]}{\sum_{i=1}^{n} w(i,j)}, \quad (1)$$

where j is an index referring to the pixels in AOD_{OK}, and $w(i,j)$ is defined as:

$$w(i,j) = \max\left(0, \frac{R^2 - d_{i,j}^{\,2}}{R^2 + d_{i,j}^{\,2}}\right), \quad (2)$$

where $d_{i,j}$ is the distance between points i and j, and R is the influence radius beyond which the observations have no weights. In this study, and based on the semivariograms calculated for the OK interpolation, we chose R=2°. As a result of this analysis, the gridded AOD at 550 nm at the validation sites matches the measured values, so that the local AOD bias at these sites is effectively removed and the error can be mostly attributed to the model rather than to the inputs.

In order to apply Eq. (1) in practice, we had to average the instantaneous AOD data measured at the experimental sites to daily values. We used a weighted average with weights $w_t = I_{0h,t}/\Sigma_l I_{0h,l}$, where $I_{0h,t}$ is the extraterrestrial irradiance on a horizontal surface at time t. The sum extends to all the values throughout each day. Those data points corresponding to a higher incoming extraterrestrial irradiance get a greater weight. Figure 2 shows the resultant gridded AOD for July 27, 2009, after application of the Cressman analysis procedure. Circles highlight the influence radius of the observations. Note the high overestimation of the MODIS L3 AOD at 550 nm over the southwest US region and how it is locally corrected by the scheme described above.

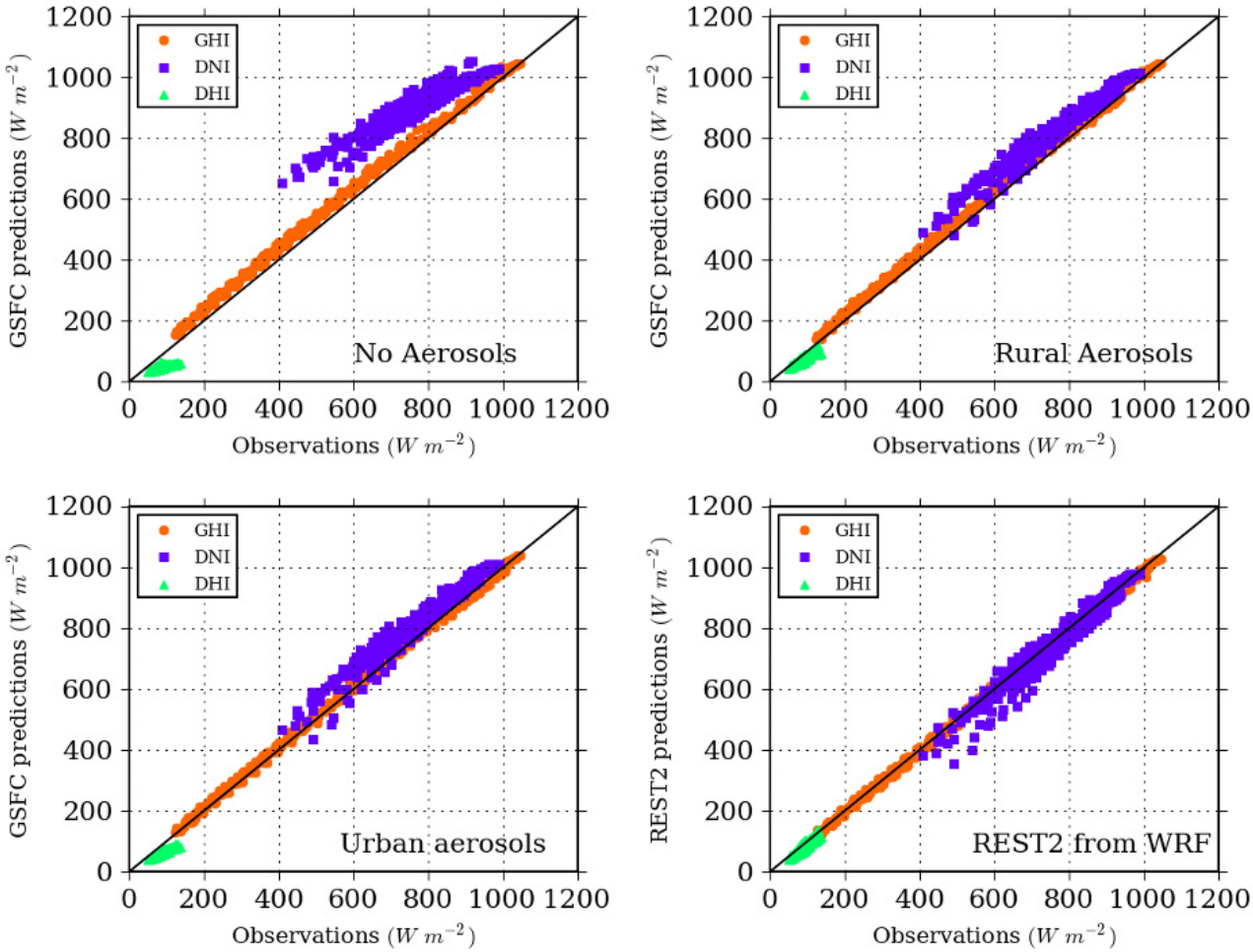

Fig. 3: Modeled GHI, DNI and DHI values against measured data at Bondville for: no aerosols, rural aerosol type, urban aerosol type, and for the REST2 model using inputs derived from the output of the WRF model.

Finally, the skill of the GSFC shortwave scheme was compared against simulations obtained with the REST2 broadband cloudless-sky model [19] at the experimental sites. This model is known for its exceptional performance, as a result of numerous experiments using inputs of the highest reliability at first-class radiometric stations worldwide [20]. The main atmospheric inputs to REST2 are site pressure, ozone amount, total nitrogen dioxide amount and, more importantly, precipitable water and turbidity coefficients (Angström exponent and AOD at 1000 nm). In order to use REST2 with an atmosphere as similar as possible to the atmosphere "seen" by the GSFC model, we gathered AOD at 550 nm, precipitable water and surface pressure from the WRF output. The Angström exponent value was set to 1.3 and was also used to derive AOD at 1000 nm from the AOD at 550 nm used in WRF. The model's default values were used for the remaining input parameters

5. RESULTS

Solar radiation components are recorded every minute at the experimental sites, but the output of WRF was only saved every 10 minutes. Consequently, only those experimental records matching the output times of WRF and under cloudless conditions in both the observations and WRF were used. Figures 3 and 4 show the modeled values (GHI, DNI and DHI) against the measured values at Bondville and Desert Rock, respectively. Bondville has a mean AOD at 550 nm of 0.17 and a mean precipitable water of 2.74 cm. In the case of Desert Rock, the mean AOD is 0.09 and the mean precipitable water is 1.54 cm. At both sites, and as expected, the GSFC scheme with no aerosols yielded a very large overestimation of DNI and, to a lesser extent, of GHI. Conversely, DHI was underestimated. However, the inclusion of the new aerosol parameterization considerably improved the results when using rural aerosols and, even more so, when using the urban type. The best results, especially for DNI and DHI, were obtained with REST2. This means that there is room for further improvements with the GSFC scheme. Similar results were obtained at Boulder, where the mean AOD is 0.13 and the mean precipitable water is 1.13 cm.

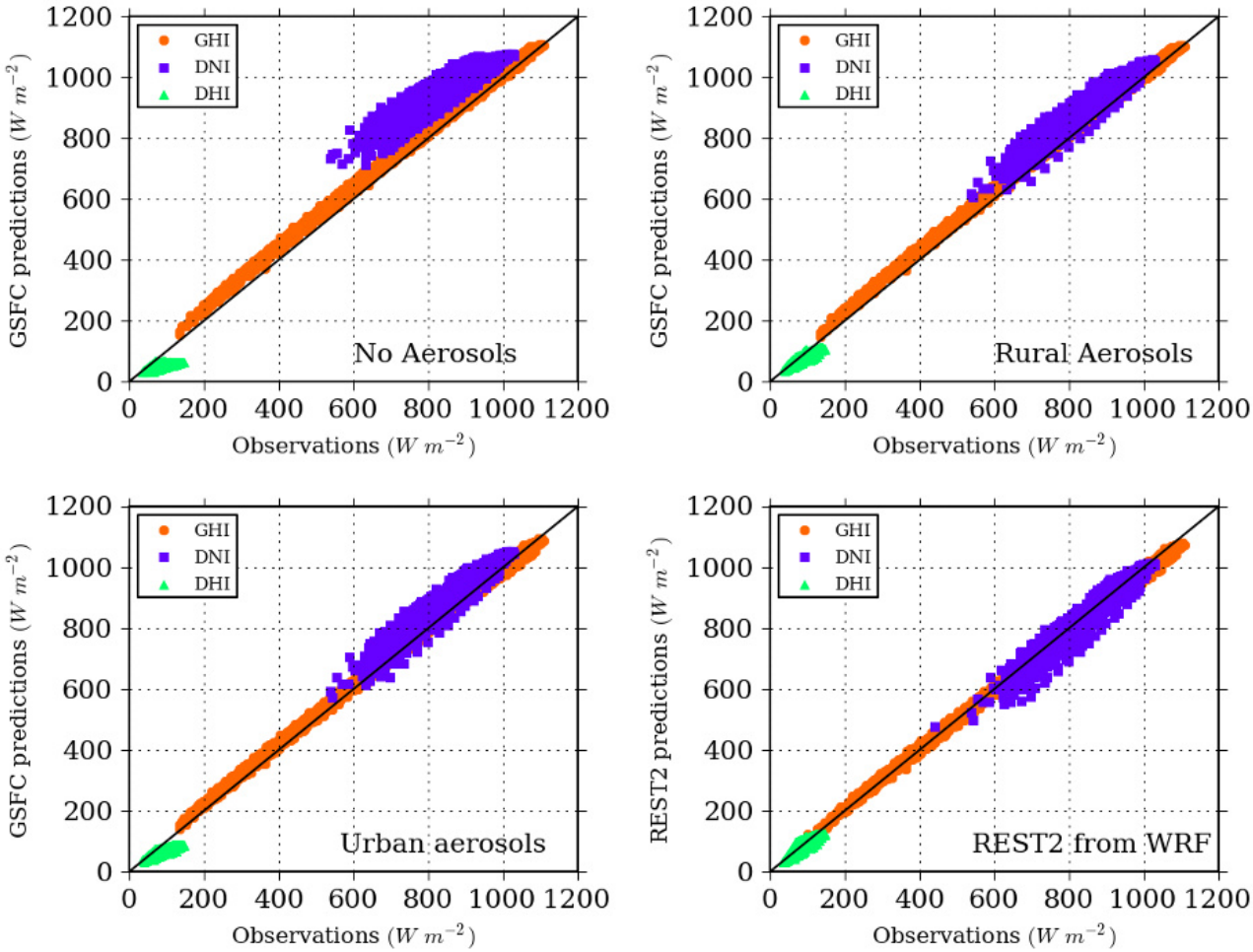

Fig. 4: As Fig. 3 but for Desert Rock.

Table 1 provides the mean bias error (MBE) and root mean square error (RMSE) for the four cases shown in Figs. 3 and 4 at the three test sites. Also shown are the skill scores of the GSFC scheme and REST2. These scores are calculated from the absolute MBE (SS_{MBE}) and from the RMSE (SS_{RMSE}), taking the case with no aerosols as reference, such as:

$$SS_{MBE} = 1 - \frac{|MBE|}{|MBE_{ref}|}, \quad (3)$$

$$SS_{RMSE} = 1 - \frac{RMSE}{RMSE_{ref}}, \quad (4)$$

where MBE_{ref} and $RMSE_{ref}$ are the MBE and RMSE of the reference model, respectively. These skill scores represent the relative improvement gained with respect to the reference case.

Overall, the inclusion of the aerosol parameterization allows large reductions in the GSFC scheme's overestimation of GHI and DNI (sometimes bringing these modeled components within or close to the uncertainty limits of the measurements), and underestimation of DHI. In the case of GHI, the MBE was reduced to less than 5%, and the improvement is comparable to that of REST2 when using the urban aerosol type (SS_{MBE}≈80%). Both cases result in a MBE of ≈1% for the three test sites. The RMSE was reduced down to ≈5% with the rural type and ≈2% with the urban type. These results are again very similar to those obtained with REST2.

The relative improvement in the estimation of the solar radiation components considered separately was smaller, yet still high. This denotes the greater difficulty of this kind of estimation. Overall, the MBE reduction in DNI was about 50% (resulting in MBE≈8%) when using a rural aerosol type, whereas the improvement was about 60% (resulting in MBE≈6%) when using an urban type. In contrast, REST2 yielded a rather insignificant underestimation of DNI, below 1% at Boulder and Desert Rock. The random errors, measured by RMSE, were acceptable in all cases: ≈8% using a rural type, ≈7% using the urban type, and ≈3% with the REST2 model.

Diffuse irradiance is probably the most difficult component to model. Even though the relative errors are high, the absolute values (in W/m^2) are of smaller magnitude than those pertaining to DNI. Again, the consideration

of the aerosol parameterization yielded large improvements in both MBE and RMSE: ≈70% with the rural type and ≈40% with the urban type. The improvement with REST2 was even larger, ≈85% for MBE and ≈70% for RMSE.

6. CONCLUSION

The use of an aerosol parameterization providing a good approximation of the optical properties of aerosols relevant for radiative transfer in the atmosphere from the AOD at 550 nm and the predominant type of aerosol has proven to be very effective in the reduction of the bias of the estimates of GHI, DNI and DHI computed with the GSFC shortwave scheme as implemented in the regional WRF model. However, the comparison of these results with those of the high-performance broadband cloudless-sky REST2 model reveal that further improvements may be achieved.

In the future, the vertical and spectral distribution of aerosols in the atmosphere will be studied in more detail. The use of potentially more accurate shortwave radiative transfer schemes in the WRF model will also be explored. Finally, this study will be extended to include all seasons and different years so as to better describe the model skills. The improvement of the radiative model skill will also benefit the predicting skills of WRF with regard to the solar radiation components, for their forecast of up to a few days.

TABLE 1: MBE, RMSE AND SKILL SCORES FOR THE VALIDATION SITES AND TEST CASES.

GHI

MBE	No-aerosol		Rural			Urban			REST2		
	Wm^{-2}	%	Wm^{-2}	%	SS	Wm^{-2}	%	SS	Wm^{-2}	%	SS
Bondville	35	6.6	23	4.4	34	8	1.5	77	-6	-1.1	83
Boulder	46	7.1	33	5.1	29	8	1.3	82	-8	-1.1	84
Desert Rock	33	4.6	25	3.5	23	8	1.1	77	-7	-1.0	78
RMSE											
Bondville	38	7.0	25	4.7	33	14	2.5	64	12	2.3	67
Boulder	47	7.3	34	5.3	28	12	1.9	74	13	1.9	73
Desert Rock	36	5.0	28	3.9	22	17	2.4	53	16	2.3	55

DNI

MBE	No-aerosol		Rural			Urban			REST2		
	Wm^{-2}	%	Wm^{-2}	%	SS	Wm^{-2}	%	SS	Wm^{-2}	%	SS
Bondville	134	17.3	61	7.9	54	48	6.2	64	-14	-1.8	90
Boulder	159	18.8	79	9.3	50	60	7.1	62	-7	-0.8	96
Desert Rock	108	12.2	58	6.6	46	48	5.4	56	-5	-0.6	95
RMSE											
Bondville	143	18.5	66	8.5	54	54	7.0	62	33	4.2	77
Boulder	163	19.3	82	9.7	50	64	7.6	61	29	3.4	82
Desert Rock	113	12.8	62	7.0	45	52	5.9	54	22	2.5	80

DHI

MBE	No-aerosol		Rural			Urban			REST2		
	Wm^{-2}	%	Wm^{-2}	%	SS	Wm^{-2}	%	SS	Wm^{-2}	%	SS
Bondville	-39	-43.9	-16	-18.5	58	-25	-28.3	35	-8	-8.8	80
Boulder	-38	-45.7	-7	-8.2	82	-21	-24.6	46	4	4.9	89
Desert Rock	-30	-35.4	-7	-7.9	78	-18	-20.7	42	2	2.4	93
RMSE											
Bondville	41	46.4	18	20.2	57	27	30.0	35	11	12.8	72
Boulder	41	48.3	10	12.3	74	23	27.3	43	11	13.2	72
Desert Rock	34	40.1	11	13.0	68	21	25.0	38	11	12.7	68

7. ACKNOWLEDGEMENT

This work was supported by a Marie Curie International Outgoing Fellowship within the 7th European Community Framework Programme, and by the University of Jaén and Caja Rural de Jaén under project R1/13/2010/01. The authors would also like to thank NOAA for providing public access to the SURFRAD

dataset, and the MODIS Science Team for the processing and public availability of the Collection 5.1 Level 3 aerosol products.

8. REFERENCES

(1) Cebecauer T., Perez R., Suri M., Comparing performance of SolarGIS and SUNY satellite models using monthly and daily aerosol data, Proceedings of the ISES Solar World Congress, Kassel, Germany, 2011.

(2) Gueymard, C., Temporal variability in direct and global irradiance at various time scales as affected by aerosols, Solar Energy, In press, 2012.

(3) Holben, B. N., Eck, T. F., Slutsker, I., Tanre, D., Buis, J. P., Setzer, A., et al.: AERONET – A federated instrument network and data archive for aerosol characterization, Remote Sens. Environ., 66, 1–16, 1998.

(4) Hubanks, P. A., King, M. D., Platnick, S., R. Pincus, MODIS Algorithm Theoretical Basis Document No. ATBD-MOD-30 for Level-3 Global Gridded Atmosphere Products (08_D3, 08_E3, 08_M3) Collection 005 Version 1.1, 2008.

(5) Morcrette J. et al., Aerosol analysis and forecast in the ECMWF Integrated Forecast System: Forward modeling, J. Geophys. Res., 114D, doi:10.1029/2008JD011235, 2009.

(6) Skamarock, W. C., et al., A description of the Advanced Research WRF version 3, NCAR Tech. Rep. TN- 4751STR, 2008.

(7) Dudhia, J., Numerical study of convection observed during the winter monsoon experiment using a mesoscale two-dimensional model, J. Atmos. Sci., 46, 3077–3107.

(8) Chou M. D., Suarez, M. J., An efficient thermal infrared radiation parameterization for use in general circulation models, NASA Tech. Memo. 104606, 3, 1994.

(9) Morcrette, J. J., Barker, H. W., Cole, J. N. S., Iacono, M. J., Pincus, R., Impact of a new radiation package, McRad, in the ECMWF Integrated Forecast System, Mon. Wea. Rev., 136, 4773-4798, 2008.

(10) Hess, M., Koepke, P., Schult, I., Optical Properties of Aerosols and Clouds: The Software Package OPAC, Bull. Amer. Meteorol. Soc., 70, 831-844, 1998.

(11) Gueymard, C., Simple Model of the Atmospheric Radiative Transfer of Sunshine, version 2 (SMARTS2): Algorithms description and performance assessment. Report FSEC-PF-270-95, Florida Solar Energy Center, 1995.

(12) Shettle, E. P., Fenn, R. W., Models for the aerosols of the lower atmosphere and the effects of humidity variations on their optical properties, Rep. AFGL-TR-79-0214, Air Force Geophysics Lab., Hanscom, MA, 1979.

(13) Levy, R. C., Remer, L. A., Kleidman, R. G., Mattoo, S., Ichoku, C., Kahn, R., Eck, T. F., Global evaluation of the Collection 5 MODIS dark-target aerosol products over land, Atmos. Chem. Phys., 10, 10399-10420, 2010

(14) Anderson, T. L., Charlson, R. J., Winker, D. M., Ogren, J. A., Holmen, K., Mesoscale variations of tropospheric aerosols, J. Atmos. Sci., 60, 119 – 136, 2003.

(15) Long, C.N., Ackerman, T.P., Identification of clear skies from broadband pyranometer measurements and calculation of downwelling shortwave cloud effects. J. Geophys. Res., 105D, 15609–15626, 2000.

(16) Dee, D. P. et al., The ERA-Interim reanalysis: configuration and performance of the data assimilation system, Q. J. R. Meteorol. Soc., 137, 553–597, 2011.

(17) Cressie, N., Statistics for Spatial Data, Revised Edition. New York, John Wiley & Sons, 1993.

(18) Daley, R., Atmospheric Data Analysis. Cambridge Atmospheric and Space Science Series, Cambridge University Press, 1991.

(19) Gueymard, C. A., REST2: High-performance solar radiation model for cloudless-sky irradiance, illuminance, and photosynthetically active radiation – Validation with a benchmark dataset, Sol. Energy, 82, 272-285, 2008.

(20) Gueymard, C. A., Clear-sky irradiance predictions for solar resource mapping and large-scale applications: Improved validation methodology and detailed performance analysis of 18 broadband radiative models, Sol. Energy, In press, 2012.